Evaluate the Humidity Sensing Properties of a CNTs/Co3O4 Nanorods Composite

Walaa M. Taha
Ain Shams University
Mohamed Morsy (83morsy@gmail.com)
Housing & Building National Research Center (HBRC) https://orcid.org/0000-0002-0019-2773
Nadra A. Nada
Ain Shams University
Medhat Ibrahim
Ain Shams University

Research Article

Keywords: Carbon nanotubes, Humidity sensor, nanocomposite, thermal analysis

Posted Date: May 20th, 2021

DOI: https://doi.org/10.21203/rs.3.rs-532253/v1

Abstract

For the development of humidity sensors, MWCNTs/Co_3O_4 nanocomposite has been prepared by precipitation method. in order to evaluate the prepared materials quality both of functionalized MWCNTs and decorated CNTs characterized by X- ray powder diffraction (XRD) ,High resolution transmission electron microscope (HRTEM) Thermal analysis (DTA and TGA) FTIR and finally Raman spectroscopy. Meanwhile the humidity sensing behavior has been also investigated. The proposed composite has been tested in the wide range in relative humidity and tesing frequency. The obtained results confirmed that the optimum testing frequency is 100 Hz. The MWCNTs/Co_3O_4 nanocomposite exhibited a good sensitivity toward humidity from11% up to 97% RH with reasonable response and recovery time. Also the sensor revealed a low hysteresis and good repeatability with increasing and decreasing of humidity levels.

1. Introduction

Relative humidity is one of the most important physical parameters that must be measured accurately because of its important effects on many vital functions of living organisms as well as industry. The measurement of relative humidity depends mainly on the use of certain functional materials that suffer from change in their physical properties when the surrounding humidity changes [1]–[7]. Metal oxide Semiconductors (MOS) are one of the most important materials used in measuring humidity, due to the low price and ease of synthesizing them in different morphologies[8][9]. A carbon nanotube is one of the most interesting materials that have been discovered yet. Since their discovery, it subjected to detailed studies to explore its fundamental properties and finding the most possible applications. CNTs have a good reputation in scientific society due to its outstanding physical and chemical properties. These outstanding properties are attributed to their unique geometric structure beside electronic and phonon structure [10][11][12][13][14]. CNTs can be better visualized as a rolled up graphene sheet in the form of a hollow nanometer tube. Two main types of CNTs can be recognized based on the numbers of concentric tube. Single wall carbon nanotubes (SWCNTs) consist of a single sheet of graphene rolled up into a single nano scale tube; while multi wall carbon nanotubes (MWCNTs) is consist of multiple concentric tubes [15] [16]. CNTs can be synthesized by various methods while the most well established methods comprise arc discharge, laser ablation and chemical vapor deposition (CVD). Among all of these methods, CVD is most suitable and forward technique. The CVD method involves growth of CNTs from volatile carbonaceous precursors (e.g., acetylene, ethylene, ethanol or methane) at 350 to 1150°C using either a nanoparticle as a catalyst. CVD has the advantage of being very flexible for modifications and easy to scale [17][18][19][20]. In spite of unique properties of CNTs, their surface needs to be modified to enhance its chemical functionality. The chemical and or physical modification generally called functionalization. This functionalization often required to enrich the performance of CNTs in different applications [21]. The functionalization of CNTs can be executed via attaching an inorganic, organic and biological functional molecule to the CNTs. Four main approaches are available for functionalizations of CNTs include endohedral filling, covalent functionalization, noncovalent functionalization and surface decoration with inorganic particles. CNTs can considered one of the best materials to use as a moisture

sensor due to their high aspect ratio. However the hydrophobic natures of CNTs hinder its ability to sense humidity. To overcome these shortage inorganic nanoparticle/CNTs have been utilized as humidity sensor [22] due to the synergistic effect coming from the integration of individual constituents. Cobalt oxide has been used in a variety of applications, including Li ion battery, catalysis and sensing [23]. Din et al investigated the humidity sensing behavior SnO_2–Co_3O_4 nanocomposites

Yadav etal fabricated an optoelectronic humidity sensor based nanostructure single layered and double layered of Co_3O_4 and $CoTiO_3$. They found that the single and double layered sensing elements of $CoTiO_3$ more sensitive than single and double layered of of Co_3O_4 [24]. Amanulla et al. prepared the β- $CoMoO_4$, Co_3O_4 through co-precipitation and solid-state method. They found that The humidity sensing measurement of composite than has been prepared by simple co-precipitation method possess highest sensitivity factor Sf = 4851 with response time of 60 s and recovery time of 230 s respectively [25]. Dai et al. produced a chemiresistive humidity sensor based on chitosan (CS)/zinc oxide/SWCNT. They found that the response of SWCNT to humidity was significantly enhanced with the help of conjugate material in the composite, particularly the CS. Also they demonstrated that the composite displayed good reproducibility [22].

In this study the MWCNTs were synthesized by CVD, and then functionalized with COOH group to reduce its hydrophobicity. Co_3O_4 nanoparticles were grafted onto the outer surface of CNTs by via simple precipitation rout. Beside this the response of CNTs/Co_3O_4 composited to humidity was investigated in a wide range of humidity (11% – 97%).

2. Experimental

2.1 Materials:

Cobalt Nitrate hexa hydrate [Co $(NO_{3)2}$. $6H_2O$] was purchased from ALPHA CHEMICA, Iron Nitrate Nona hydrate [Fe $(NO_3)_2$.$9H_2O$ was obtained from Guangdong Guangzhou Chemical Factory Co, Ltd. Magnesium Oxide MgO (PROLABO Company, purity 99%). sulfuric acid H_2SO_4 was obtained from (Scharlau, European Union, purity 95-98%), nitric acid (HNO_3) (Caroler, European Union, 69.5%). Urea was purchased from El-Nasr Pharmaceutical Company, Egypt

2.2 MWCNTs synthesizing and purifications:

Bimetallic Fe/Co supported over MgO has been prepared by impregnation method and utilized as a catalyst for MWCNTs synthesizing. All chemicals were used as it is without any further purification. In brief 3.62g of Fe $(NO_3)_2$.$6H_2O$ and 2.47g of Co $(NO_3)_2$.$9H_2O$ were dissolved in 50 ml of distilled H_2O then 10g of MgO added slowly during continuous stirring. The resultant composite was calcined at 500^oC for 2 hrs, and then crushed with agate pestle to be fine powder. The MWCNTs was deposited over Bimetallic Fe/Co catalyst at 750^oC using acetylene and nitrogen as carbon source and carrier gas respectively. To purify MWCNTs, a proper amount of as synthesized MWCNTs was refluxed in a 3:1 mixture of

concentrated $H2_SO_4$ and HNO_3 solution. More details regarding synthesizing, purification and functionalization of MWCNTs can be found in our previous reported work [26], [27].

2.3 Decorating MWCNTs with Co_3O_4

Cobalt oxide (Co_3O_4) nanoparticles were anchored onto the outer surface of MWCNTs using hydrothermal rout. firstly 40mg of MWCNTs were dispersed in 30ml of distilled water by ultrasonic homogenizer for 30min. 300 mg of cobalt nitrate hexa hydrate was added to MWCNTs suspension under continuous stirring, and then 300mg of urea was added, the mixtures were allowed to stir for additional 2 hr. The solution was transferred into a 50ml Teflon-lined sealed stainless steel autoclave and maintained at 150^oC under autogenous pressure for 4hr. the MWCNTs decorating process is illustrated in fig. 1.

2.4 Characterization techniques

-The shape and size of purified MWCNTs and Co_3O_4/MWCNTs nanocomposite were examined by high resolution transmission electron microscope (HRTEM) JEM-2100. The crystalline structure was determined by XRD diffractometer with a secondary monochromatic wavelength of Cu (λ=1.542A^o) at 45 K.V., 35mA, and scanning speed of 0.02/sec. Thermal gravimetric analysis (TGA) measurements were obtained by STDQ-600 thermal analyzer from room temperature up to 1000^{o}C under air atmosphere. The FTIR spectroscopy has been utilized to diagnose the functional groups on the surface of purified MWCNTs and the functional groups of nanoparticles on the purified MWCNTs. the spectra were collected by (FTIR Vertex 70 Bruker optic model device). Raman spectroscopy has been utilized to observe the structure and SP^2 hybridization. The spectra were collected by (Bruker SENTERRA) with a (ND-YAG) laser source and with wavelength of 532nm.

2.5 Sensor fabrication:

A humidity sensor was developed over fluorinated tin oxide (FTO) coated glass substrate. 5mg of Co_3O_4/MWCNTs and 5 ml of distilled water were mixed with agate pestle to form a paste. A small amount of a paste was applied on the surface of FTO and then, the device was dried at 60 °C until complete evaporation of water. Subsequently the sensor was aged at 1 V and 1 kHz for 36 h to enhance its stability as shown in fig. 2. A saturated solution of LiCl, $C_2H_3KO_2$, NaCl, KCl and K_2SO_4 were utilized to develop a standard level of humidity as shown in table 1.

Table1: The relative humidity of saturated salt solutions

saturated solutions	% RH
LiCl	11
$C_2H_3KO_2$	43
NaCl	75
KCl	85
K_2SO_4	97

The humidity sensor was dispersed in this different values of humidity level from low %RH value to high %RH and by HOKI LCR bridge the real time impedance was recorded with AC-1V with changing frequency from 50Hz to 1000KHz to calculate the impedance values which giving more results. Also studying the response-recovery time of Co_3O_4/MWCNTs sensor from low %RH =11% to %RH=43% and repeating between 11% and the other higher value.at constant frequency. The setup of sensing experiment was shown in figure 2b

3. Results And Discussion

High Resolution Transmission Electron Microscope (HRTEM) images of fig.3a clarified that the purified MWCNTs have a hollow cylindrical shape and are free from the presence of any impurities, and amorphous carbons. Both the inner and outer diameter of MWCNTs were measured directly from HRTEM image and found to be 6 nm and 26 nm respectively. Figure 3b displays the HRTEM image of Co_3O_4/MWCNTs nanocomposite. It is obvious that the Co_3O_4 are of nanorods form with noticeable agglomeration. The outer diameter of Co_3O_4 nanorods have been measured to be about 49nm.

The XRD diffraction peaks of purified MWCNTs and Co_3O_4/MWCNTs are shown in figure 4. It was observed that all the peaks have high intensity indicating that the samples have good crystallinity. The characteristic diffraction peaks at $2\theta=26.6^o$ and 44.7^o are indexed to (002) and (102) planes of the graphite confirming the formation of MWCNTs as assigned earlier. The diffraction peaks at 19^o, 31^o, 37^o, $59.^o$ and 65^o are indexed to (220), (311), (222), (400), (422) and (511) reflections of Co_3O_4 naorods respectively. No other diffraction peaks have been observed for other impurities [28]. The crystallite size (D) of Co_3O_4 nanoparticles have been calculated from XRD by Debye Sheerer Equation [5]:

$$D=K\lambda/\beta\cos\theta \qquad [1]$$

Where λ is the wave length, θ is the diffraction angle, and β is the peak width at half maximum. The size of cubic cobalt oxide is determined to be about 50nm which confirm the result obtained from HRTEM.

In order to estimate the thermal stability and existance the Co_3O_4 nanorods, the samples have been subjected to controlled heating, hence the coresponding DTA and TGA curves have been obtained. The

sampes were heated up from room temperature up to 800^{o}C in air with heating rate of 20^{o}C/min. The TGA thermograme of purified MWCNTs exhibts a wieght loss at 650^{o}C corresponding to 93.5 wt% which attributed to the degradation of the MWCNTs. In case of Co_3O_4/MWCNTs two weight loses have been recognized. Beside the peak of MWCNTs; an additional peak at 328^{o}C has been observed as shown in fig. 5a. The presence of urea $CO(NH_2)_26H_2O$ in preparation of cobalt oxide is mostly important because it decompose under heat and gives NH_3 and CO_2 which is the initial stage in preparation of nano particles from Cobalt hydroxy carbonate $Co_2(OH)_2(CO_3)$ then this complex decompose by heat to obtain cobalt oxide [29].

It was belvied that the thermal degradtaion of MWCNTs is directly related to defects, the less the defects, the higher the decomposition temperature [30]. The wieght loss of MWCNTs of Co_3O_4/MWCNTs was shifted by 100^{o}C. This could be due to the deformations caused by hydrothermal treatment. The DTA curves of both MWCNTs and Co_3O_4/MWCNTs are shown in fig. 5b. The DTA curve of MWCTs exhibits one exothermic peak which is attributed to nanotube consumption. In comparison with Co_3O_4/MWCNTs composite, the nanotube consumption exothermic peak was shifted to lower temperature indicating the presence of some defect due to hydrothermal treatment.

Thermal analysis is one of the important tools that has been used in the characterization of CNTs, as well as estimating the amount of metal oxides loaded on their surface, but in spite of this it cannot distinguish between species of carbon nanotubes and knows any defects act on structure and therefore, it is necessary to characterize the prepared materials using another tool.

To evaluate the functional groups on the surface of MWCNTs and the composite Co3O4/MWCNTs; FTIR spectra was used with spectra region from (4000-400cm^{-1}) as shown in figure 6. For purified MWCNTs the broud band at approximatly 3435cm^{-1} is assigend to stretching of –OH in hydroxyle and carboxyle group(C-OH,O=C-OH) [31]. The spectra bands at 2924-2858cm^{-1} are attributed to symmetric and assymmetric stretching vibration of C-H in CH_2 and $-CH_3$ group [32]. The band at 1714cm^{-1} arrtibuted to C=O present in carboxylic group [33]. the band at 1628cm^{-1} associated to carbonyle group present in ring structure and related to stretch vibration C=C of SP^2 hypridization in carbon nanotube backbone [34].the band at 1115-1060cm^{-1} refer to C-O stretching vibration in carboxylic group[32]. this results confirm on successful oxidation of MWCNTs and also for Co_3O_4/MWCNTs there are two additional sharp bands at 669and 560cm^{-1} corresponding to presence of Co^{+2} and Co^{+3} in spinal Co-O stretching vibrations where Co^{+2} related to tetrahedral coordinate and Co^{+3} to octahedral coordinate.FTIR spectra confirm presrence of Co_3O_4 structure [29].

Raman spectrometer is one of the most important characterization tools used to distinguish between different nanocarbon structures, as well as to determine the presence of deformations and also to determine the type of metal oxides on their surface. The Raman shifts of both purified MWCNTs and Co_3O_4/MWCNTs are shown in fig. 7. For purified MWCNTs three Raman shifts at 1566cm^{-1}, 1338cm^{-1},

2677cm^{-1} corresponds to G (the graphite band), D (disorder band), and G/ (second order harmonic) bands were recognized. The intensity ratio I_D/I_G is an important indicator for the precence of functional group[30] [29], [35]. The I_D/I_G was estimated to be 0.6 indicating the sucsessfully functionalization of MWCNTs. The charactrisitc Raman bands of Co_3O_4/MWCNTs observed at, 527 cm^{-1} were attributed to the F_{2g} Raman active mode, while those located at 483 and 670 were pelonging to E_g and A_{1g} modes, respectively. The highest

In order to evaluate the response of the prepared sensor toward humidity, the impedance variation of the nanocomposite was recorded at different humidity levels (11% RH – 97 % RH) and at different testing frequency (50 Hz – 100kHz). The impedance variation versus the humidity at different testing frequency is illustrated in fig. 7. It was noticed that at low frequency, the impedance decreases linearly with increasing the humidity level. With further increasing in the testing frequency, the impedance variation increases, while at higher frequency (100 kHz) the impedance variation becomes insignificant with no obvious trend. This could be explained based on the water molecules are not able to be polarized at high frequencies [5], [30].

Hence for further evaluation the testing frequency was set at 50Hz. The hysteresis effects due to the adsorption and desorption of water molecule is illustrated in fig. 8. It was observed that during the adsorption process, the impedance increases with the increase of humidity; while during desorption of the water molecule the response decreases with decrease of humidity. Since the water molecule is adsorbed physically over the surface of the sensor via hydrogen bond; so that it was expected that the hydrogen bond plays a vital role in hysteresis. In our case, there are two types of formed hydrogen bonds: bonds formed between water molecule and sensing material, and bonds between water molecules and other water molecules. During the adsorption process (humidity increment) the water molecules are physically adsorbed on the surface of the sensor via hydrogen bond. In case of desorption process (humidity decrement) the water molecules departed from the surface of the sensor which require more energy to overcome the hydrogen bonds. As was confirmed earlier, the desorption of water molecule is difficult than adsorption of water molecule, which in turn will results in hysteresis.

The impedance variation versus humidity can be fitted in a linear correlation as depicted in fig. 9. Figure 10 represents the adsorption and desorption response curves for the sensor at RH% of 75, and 97, respectively. The curves indicated excellent ability of the sensors to respond against increasing and reducing humidity levels with realistic response and recovery times.

The humidity sensing mechanism of the Co_3O_4/MWCNTs composite is explained based on the complex impedance spectroscopy (CIS) measurements. The relationship between real part of impedance (Z\) and imaginary part (Z\\) at relative humidity of 11%, 43% and 97% is illustrated in fig 11. It was observed that all curves are semicircles; also the curvature of the semicircle decreases with increasing humidity level. This means that the bulk resistance of the sensing materials decreases as humidity increases [36]. In the case of low humidity value, the concentration of the adsorbed water on the surface of the sensing material is weak. The water molecule will be absorbed on the active sites in order to form a hydroxyl

group. Therefore, the protons formed from the hydroxyl group can be transferred to form $H3O^{+}$. And although these charged ions are insufficient to cause electrical conduction, they may bend energy levels, and therefore the conduction is done through electrons. Due to the presence of MWCNTs, the transmission of electronics is easy. When the humidity increases, the conduction process takes place through the aforementioned mechanism, and this has been proven through CIS measurements.

Conclusion

In this study the possibility of using a CNTs/Co_3O_4 nanocomposite as a humidity sensor was examined. The HRTEM and XRD measurements confirmed that the Co_3O_4 nano particles formed in a crystalized form and attached to the surface of the MWCNTs. The size of cubic cobalt oxide is about 50nm as confirm HRTEM and XRD measurements. The Raman analysis confirmed the presence of D, G and G\ band as well as the characteristic bands of Co_3O_4 particles. The humidity sensing behavior confirmed that the optimum testing frequency is 100Hz. The obtained results emphasizes that the sensor has a reasonable sensitivity, low hysteresis, and good repeatability.

References

[1] N. Mohseni Kiasari, S. Soltanian, B. Gholamkhass, and P. Servati, “Room temperature ultra-sensitive resistive humidity sensor based on single zinc oxide nanowire,” *Sensors and Actuators, A: Physical*, vol. 182, pp. 101–105, 2012.

[2] T. Şaşmaz Kuru, M. Kuru, and S. Bağcı, “Structural, dielectric and humidity properties of Al-Ni-Zn ferrite prepared by co-precipitation method,” *Journal of Alloys and Compounds*, vol. 753, pp. 483–490, 2018.

[3] P. V. Adhyapak, V. Kadam, U. Mahadik, D. P. Amalnerkar, and I. S. Mulla, “Influence of Li doping on the humidity response of maghemite (γ-Fe2O3) nanopowders synthesized at room temperature,” *Ceramics International*, vol. 39, no. 7, pp. 8153–8158, 2013.

[4] C. Chen, X. Wang, M. Li, Y. Fan, and R. Sun, “Humidity sensor based on reduced graphene oxide/lignosulfonate composite thin-film,” *Sensors and Actuators, B: Chemical*, vol. 255, pp. 1569–1576, 2018.

[5] E. E. Ateia, M. M. Arman, and M. Morsy, “Synthesis, characterization of NdCoO3 perovskite and its uses as humidity sensor,” *Applied Physics A: Materials Science and Processing*, vol. 125, no. 12, pp. 1–9, 2019.

[6] M. Morsy, M. M. Mokhtar, S. H. Ismail, G. G. Mohamed, and M. Ibrahim, “Humidity Sensing Behaviour of Lyophilized rGO/Fe2O3 Nanocomposite,” *Journal of Inorganic and Organometallic Polymers and Materials*, vol. 30, no. 10, pp. 4180–4190, 2020.

[7] A. Y. Lipare, P. N. Vasambekar, and A. S. Vaingankar, “Dielectric behavior and a.c. resistivity study of humidity sensing ferrites,” *Materials Chemistry and Physics*, vol. 81, no. 1, pp. 108–115, 2003.

[8] M. Morsy, I. S. Yahia, H. Y. Zahran, and M. Ibrahim, “Hydrothermal Synthesis of CNTs/Co 3 O 4 @rGO Mesopours Nanocomposite as a Room Temperature Gas Sensor for VOCs,” *Journal of Inorganic and Organometallic Polymers and Materials*, vol. 29, no. 2, pp. 416–422, 2019.

[9] M. Velumani, S. R. Meher, and Z. C. Alex, “Composite metal oxide thin film based impedometric humidity sensors,” *Sensors and Actuators, B: Chemical*, vol. 301, no. May, p. 127084, 2019.

[10] S. Brahim, S. Colbern, R. Gump, A. Moser, and L. Grigorian, “Carbon nanotube-based ethanol sensors,” 2009.

[11] L. Pellegrino, M. Daghetta, M. Calloni, T. Dellavedova, C. Mazzocchia, and A. Citterio, “Process Optimization and Kinetic Study of Multiwalled Carbon Nanotube Synthesis,” *Chemical Engineering Transactions*, vol. 43, pp. 709–714, 2015.

[12] M. Pawlyta, L. A. Dobrzanski, W. Kwasny, C. W. Tai, A. Krzton, and B. Liszka, “Synthesis and Characterization of Carbon Nanotubes Decorated with Gold Nanoparticles,” *Acta Physica Polonica A*, vol. 118, no. 3, pp. 483–486, 2016.

[13] Q. Zhang, J. Q. Huang, M. Q. Zhao, W. Z. Qian, and F. Wei, “Carbon nanotube mass production: Principles and processes,” *ChemSusChem*, vol. 4, no. 7, pp. 864–889, 2011.

[14] X. Yuan *et al.*, “Diamond & Related Materials Low-cost synthesis of multi-walled carbon nanotubes using red soil as catalyst,” *Diamond & Related Materials*, vol. 112, no. December 2020, p. 108241, 2021.

[15] T. Maruyama *et al.*, “Vertically aligned growth of small-diameter single-walled carbon nanotubes by alcohol catalytic chemical vapor deposition with Ir catalyst,” *Applied Surface Science*, vol. 509, no. January, p. 145340, 2020.

[16] M. D. Yadav and K. Dasgupta, “Role of sulfur source on the structure of carbon nanotube cotton synthesized by floating catalyst chemical vapour deposition,” *Chemical Physics Letters*, vol. 748, no. December 2019, p. 137391, 2020.

[17] F. Farzaneh, N. F. Hamedani, and V. Daadmehr, “Preparation of Carbon Nanotubes by CVD Process over Nanoparticles of Ni-Ce-Zr Mixed Oxides,” *Journal of Sciences*, vol. 19, no. 2, pp. 119–123, 2008.

[18] E. Singh, U. Kumar, R. Srivastava, and B. C. Yadav, “Catalytic growth of MWCNT using CVD and its application as opto-electronic humidity sensor,” *Carbon Letters*, vol. 30, no. 2, pp. 215–224, 2020.

[19] J. Liu, S. Fan, and H. Dai, “Recent Advances in Methods of Forming Carbon Nanotubes,” *MRS Bulletin*, vol. 29, no. April, pp. 244–250, 2004.

[20] M. Escobar *et al.*, “Synthesis of carbon nanotubes by CVD: Effect of acetylene pressure on nanotubes characteristics,” *Applied Surface Science*, vol. 254, no. 1 SPEC. ISS., pp. 251–256, 2007.

[21] B. Song *et al.*, “Effects of hydroxyl, carboxyl, and amino functionalized carbon nanotubes on the functional diversity of microbial community in riverine sediment,” *Chemosphere*, vol. 262, p. 128053, 2021.

[22] H. Dai, N. Feng, J. Li, J. Zhang, and W. Li, “Chemiresistive humidity sensor based on chitosan/zinc oxide/single-walled carbon nanotube composite film,” *Sensors and Actuators, B: Chemical*, vol. 283, no. December 2018, pp. 786–792, 2019.

[23] A. Din *et al.*, “Impedimetric humidity sensor based on the use of SnO2–Co3O4 spheres,” *Journal of Materials Science: Materials in Electronics*, vol. 28, no. 5, pp. 4260–4266, 2017.

[24] B. C. Yadav, R. C. Yadav, S. Singh, P. K. Dwivedi, H. Ryu, and S. Kang, “Nanostructured cobalt oxide and cobalt titanate thin films as optical humidity sensor: A new approach,” *Optics and Laser Technology*, vol. 49, pp. 68–74, 2013.

[25] A. Mobeen Amanulla *et al.*, “Antibacterial, magnetic, optical and humidity sensor studies of β-CoMoO4 - Co3O4 nanocomposites and its synthesis and characterization,” *Journal of Photochemistry and Photobiology B: Biology*, vol. 183, no. April, pp. 233–241, 2018.

[26] M. Morsy, M. Helal, M. El-Okr, and M. Ibrahim, “Preparation, purification and characterization of high purity multi-wall carbon nanotube,” *Spectrochimica Acta - Part A: Molecular and Biomolecular Spectroscopy*, vol. 132, 2014.

[27] M. Morsy, M. Helal, M. El-Okr, and M. Ibrahim, “Preparation and characterization of multiwall carbon nanotubes decorated with zinc oxide,” *Der Pharma Chemica*, vol. 7, no. 10, pp. 139–144, 2015.

[28] K. Xu *et al.*, “Fabrication of novel flower-like Co3O4structures assembled by single-crystalline porous nanosheets for enhanced xylene sensing properties,” *Journal of Alloys and Compounds*, vol. 706, pp. 116–125, 2017.

[29] M. Roy, S. Ghosh, and M. K. Naskar, “Synthesis of morphology controllable porous Co3O4 nanostructures with tunable textural properties and their catalytic application,” *Dalton Transactions*, vol. 43, no. 26, pp. 10248–20257, 2014.

[30] I. S. Journal, “Graphene foam decorated with ZnO as a humidity sensor,” 2019.

[31] A. Nasiri, M. Shariaty-Niasar, A. M. Rashidi, and R. Khodafarin, “Effect of CNT structures on thermal conductivity and stability of nanofluid,” *International Journal of Heat and Mass Transfer*, vol. 55, no. 5–6, pp. 1529–1535, 2012.

[32] B. Scheibe, E. Borowiak-Palen, and R. J. Kalenczuk, “Oxidation and reduction of multiwalled carbon nanotubes - preparation and characterization,” *Materials Characterization*, vol. 61, no. 2, pp. 185–191, 2010.

[33] L. Liu, Y. Qin, Z. Guo, and D. Zhu, “<Carbon41-331.Pdf>,” vol. 41, no. August 2002, pp. 331–335, 2003.

[34] M. Varga *et al.*, “Diamond/carbon nanotube composites: Raman, FTIR and XPS spectroscopic studies,” *Carbon*, vol. 111, pp. 54–61, 2017.

[35] B. Tserengombo, H. Jeong, A. Delgado, E. Dolgor, and S. Kim, “The alkaline synthesizing method for improved thermal characteristics of CNT/alumina nanocomposite,” *Diamond and Related Materials*, vol. 109, no. May, p. 108082, 2020.

[36] K. J. Hamam and F. Salman, “Dielectric constant and electrical study of solid-state electrolyte lithium phosphate glasses,” *Applied Physics A: Materials Science and Processing*, vol. 125, no. 9, pp. 1–11, 2019.

Figures

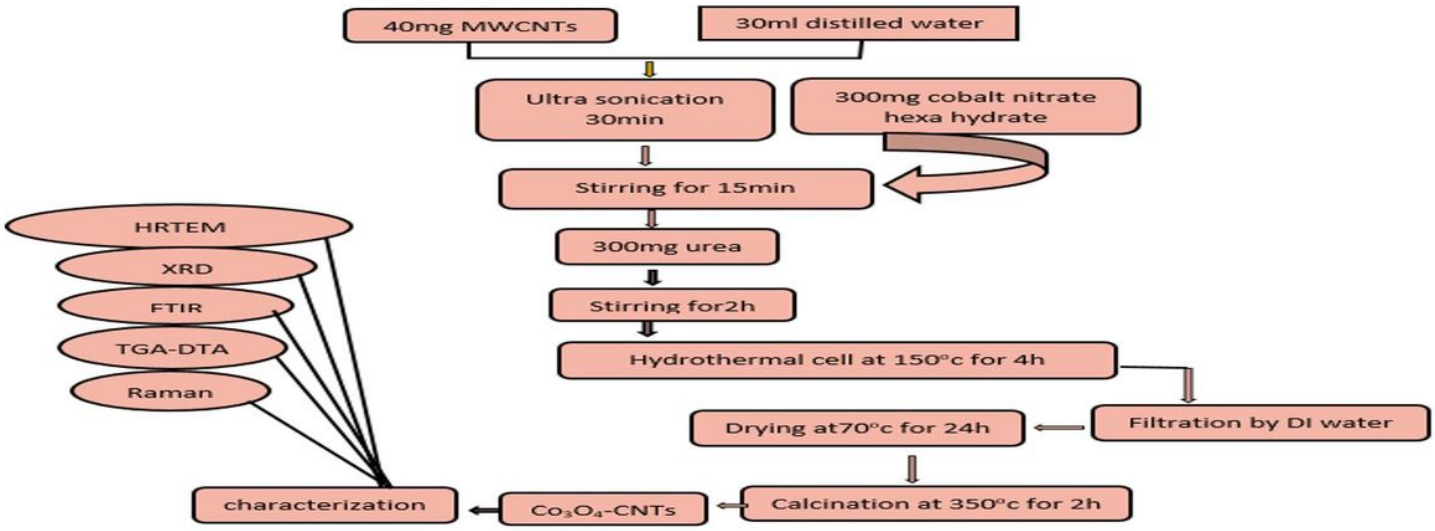

Figure 1

Synthesis process of Co3O4-MWCNTs by hydrothermal method

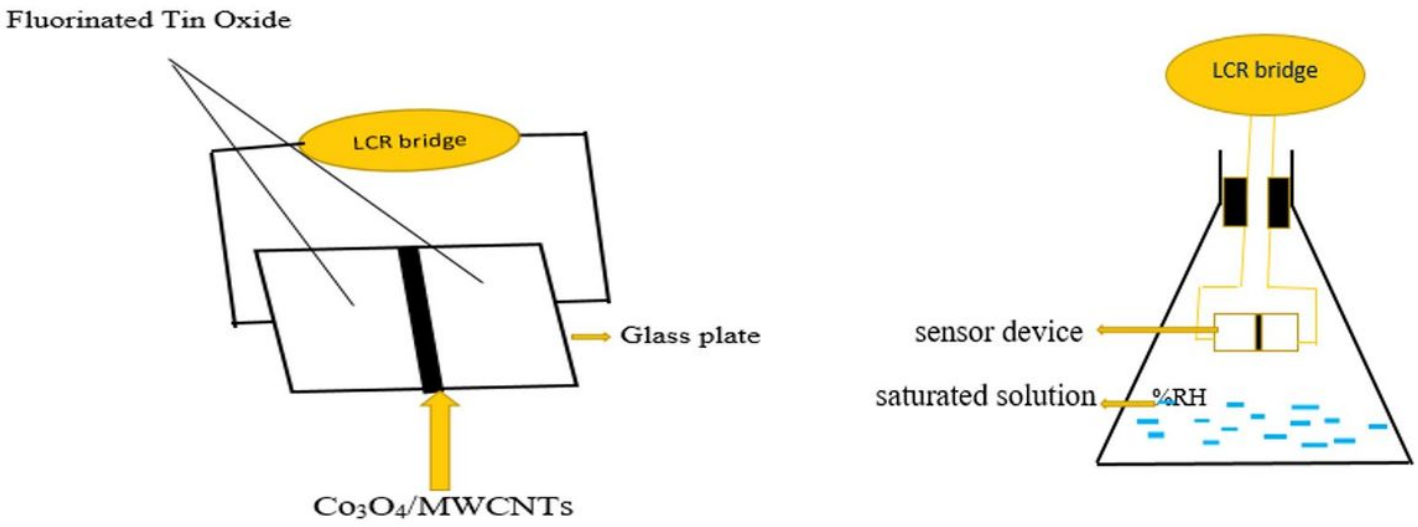

Figure 2

(a) The Co3O4/MWCNTs sensor and (b) the setup of humidity sensing measurement.

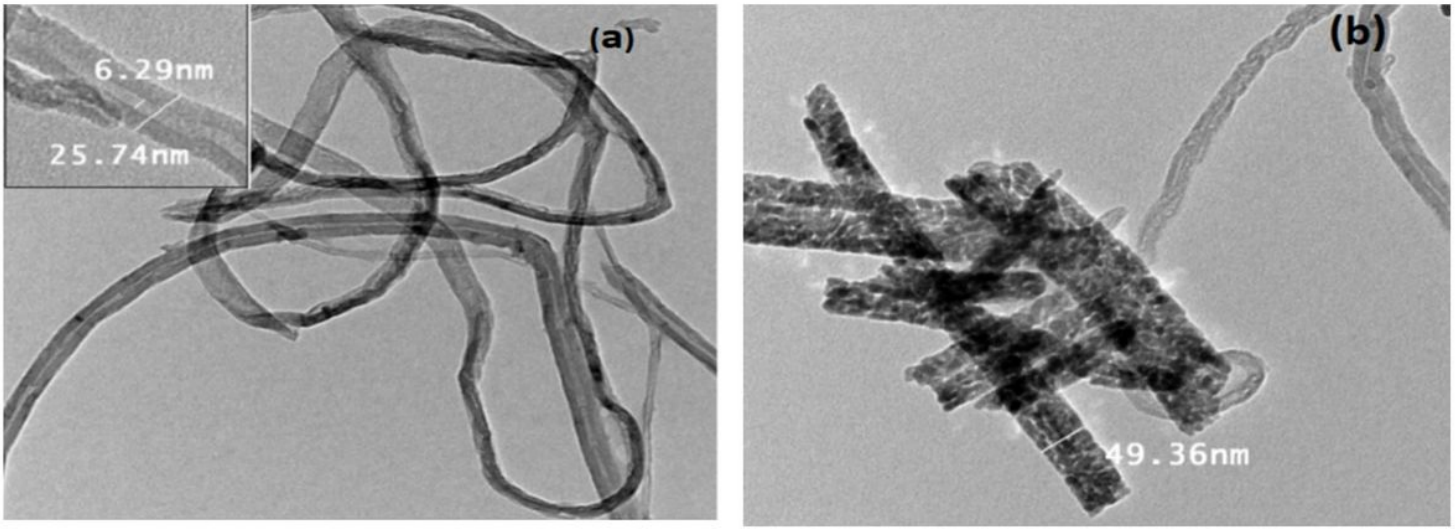

Figure 3

HRTEM of a) purified MWCNTs, and b) The Co3O4/MWCNTs nanocomposite

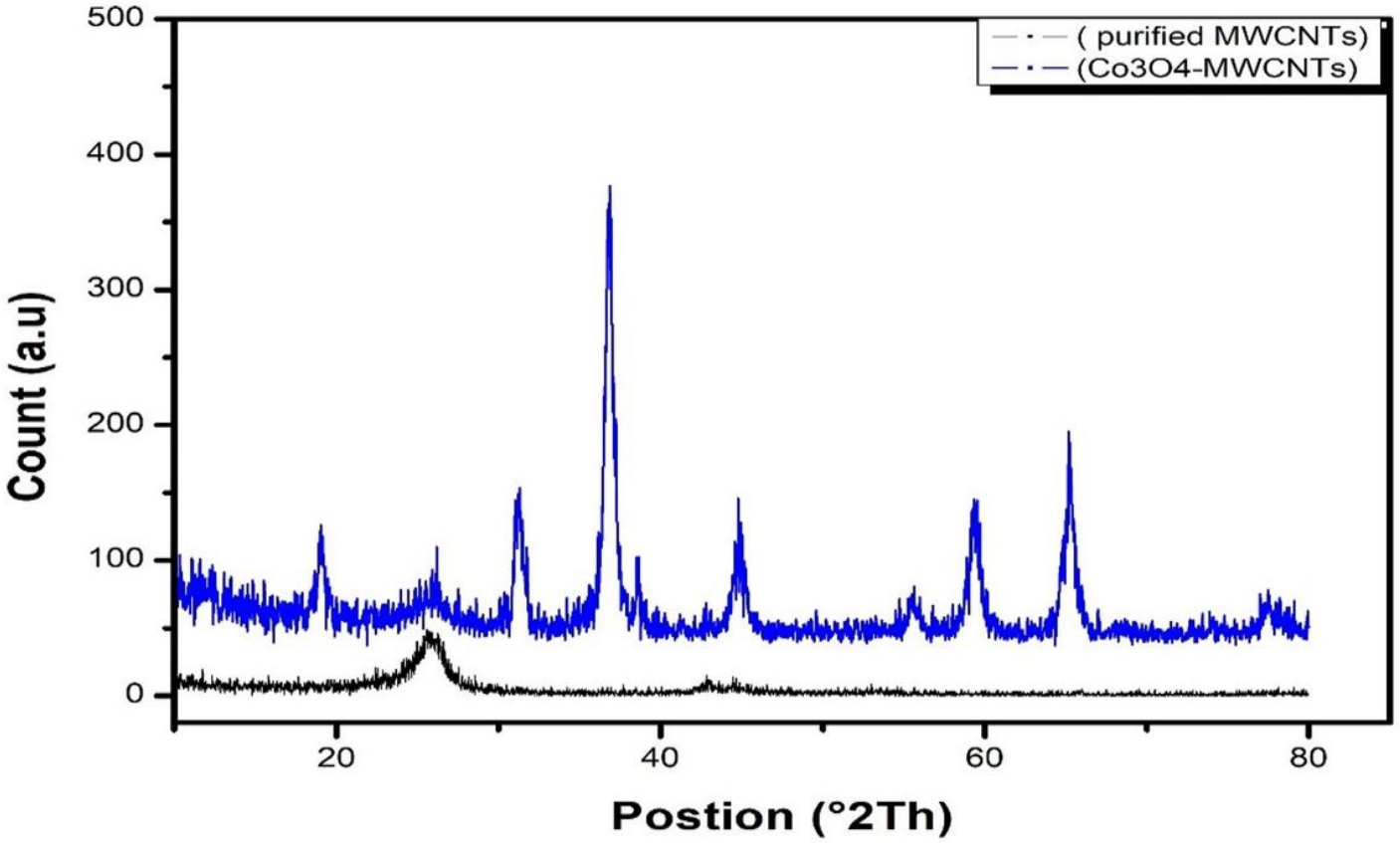

Figure 4

XRD pattern of MWCNTs and Co3O4/MWCNTs

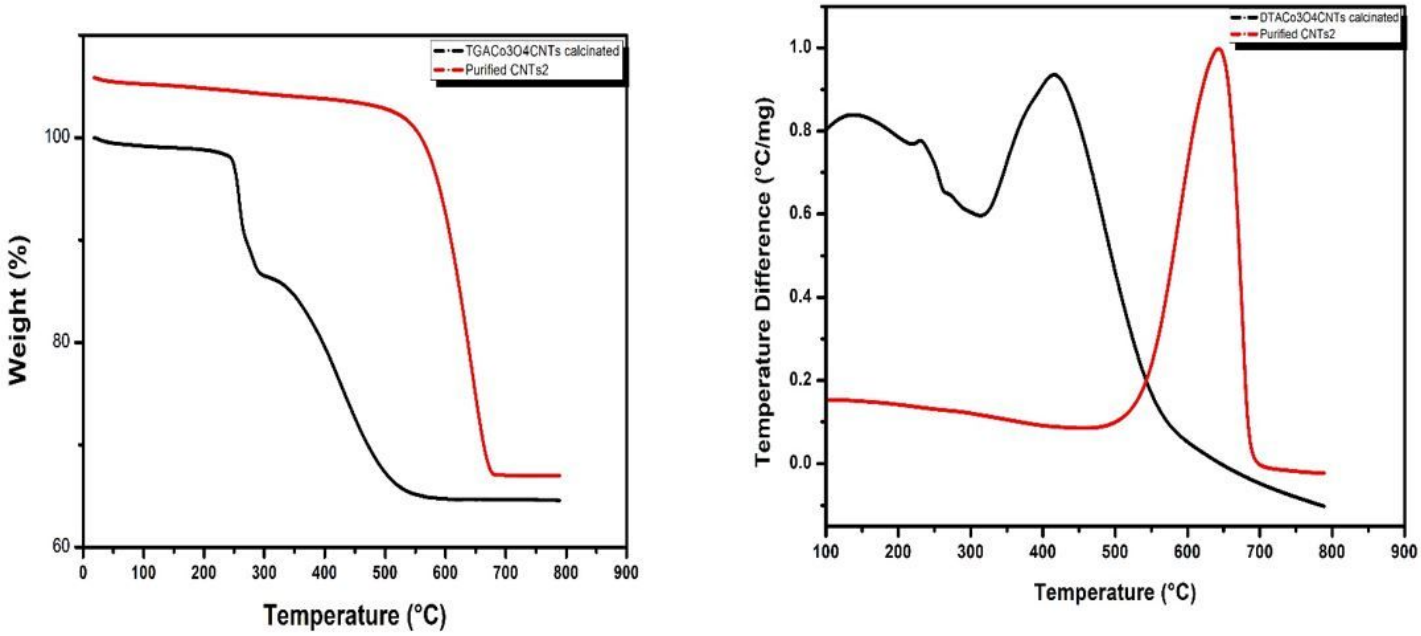

Figure 5

a: TGA thermogram of MWCNTs and Co3O4/MWCNTs composite. b: DTA thermogram of MWCNTs and Co3O4/MWCNTs composite.

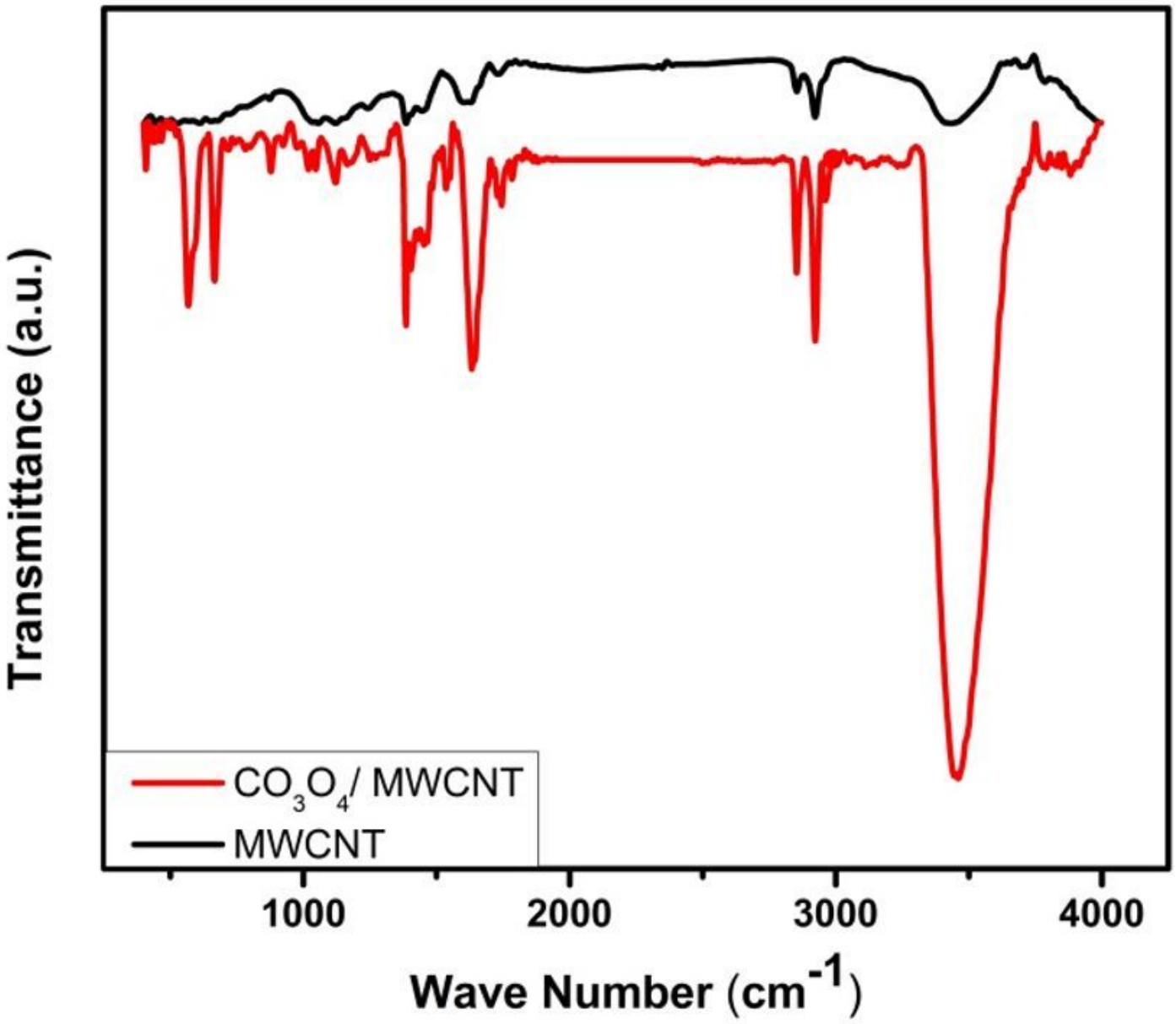

Figure 6

FTIR spectra of MWCNTs and Co3O4/MWCNTs composite

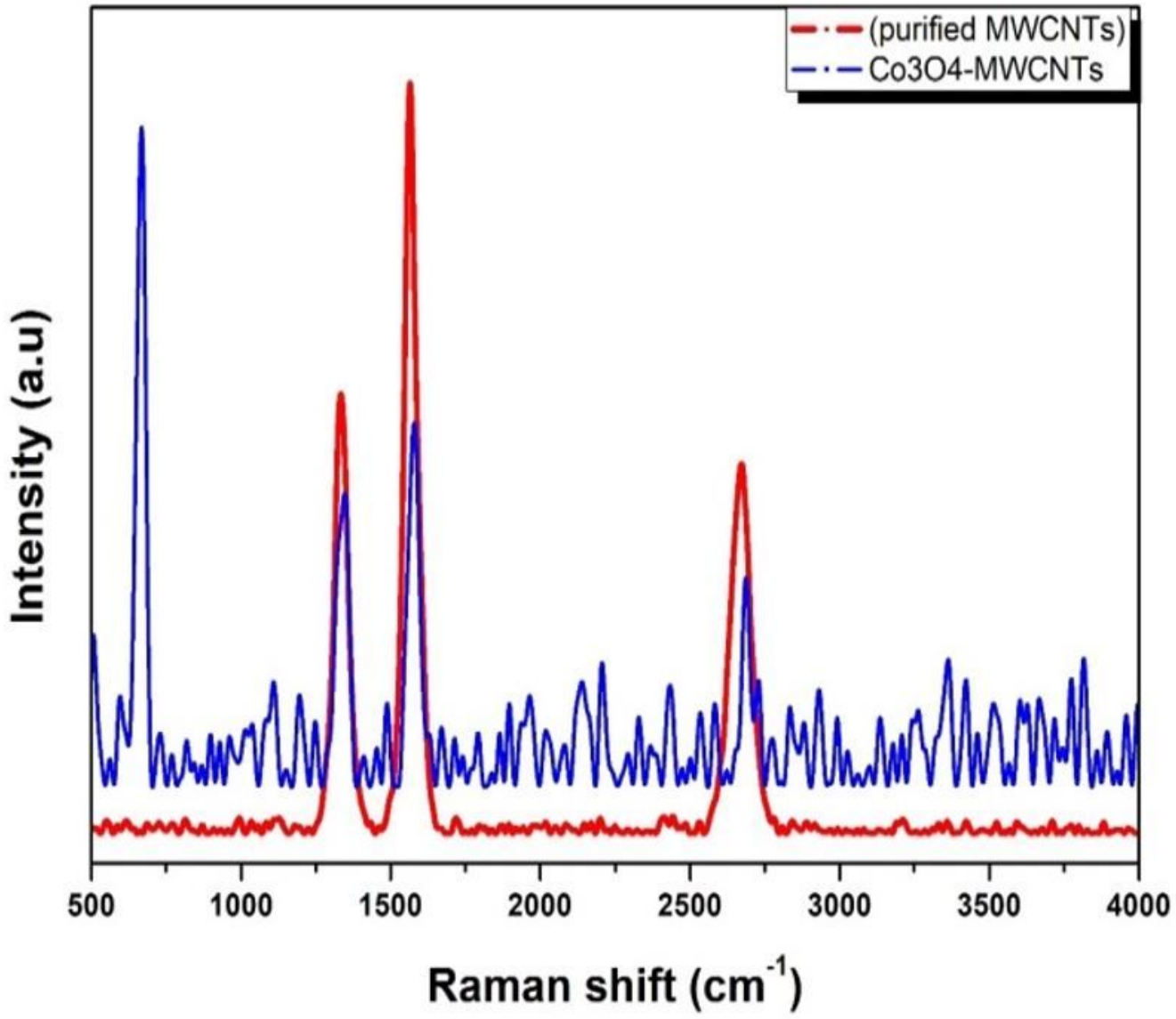

Figure 7

Raman spectra of MWCNTs and Co3O4/MWCNTs composite

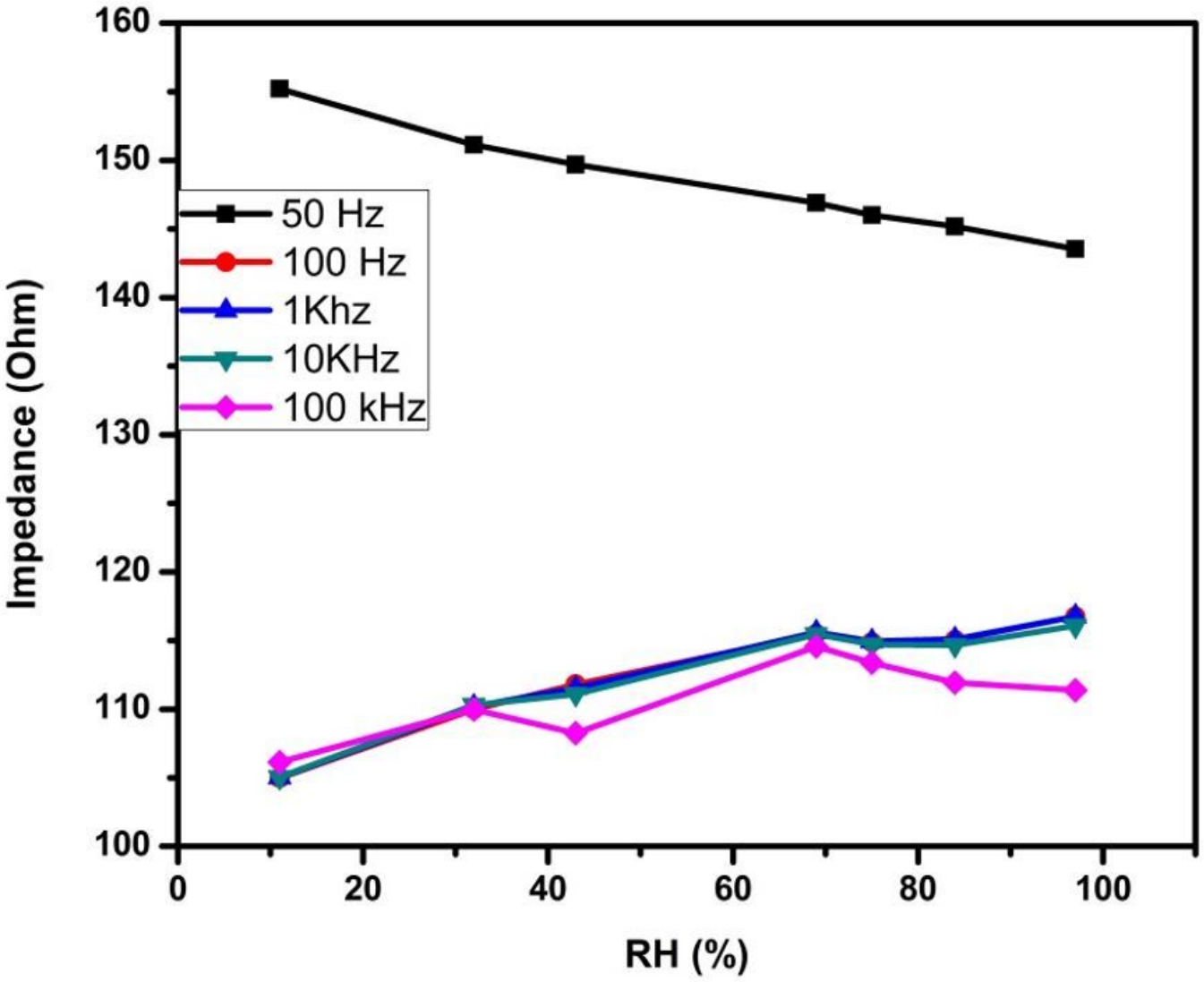

Figure 8

The impedance variation versus the humidity at different testing frequency

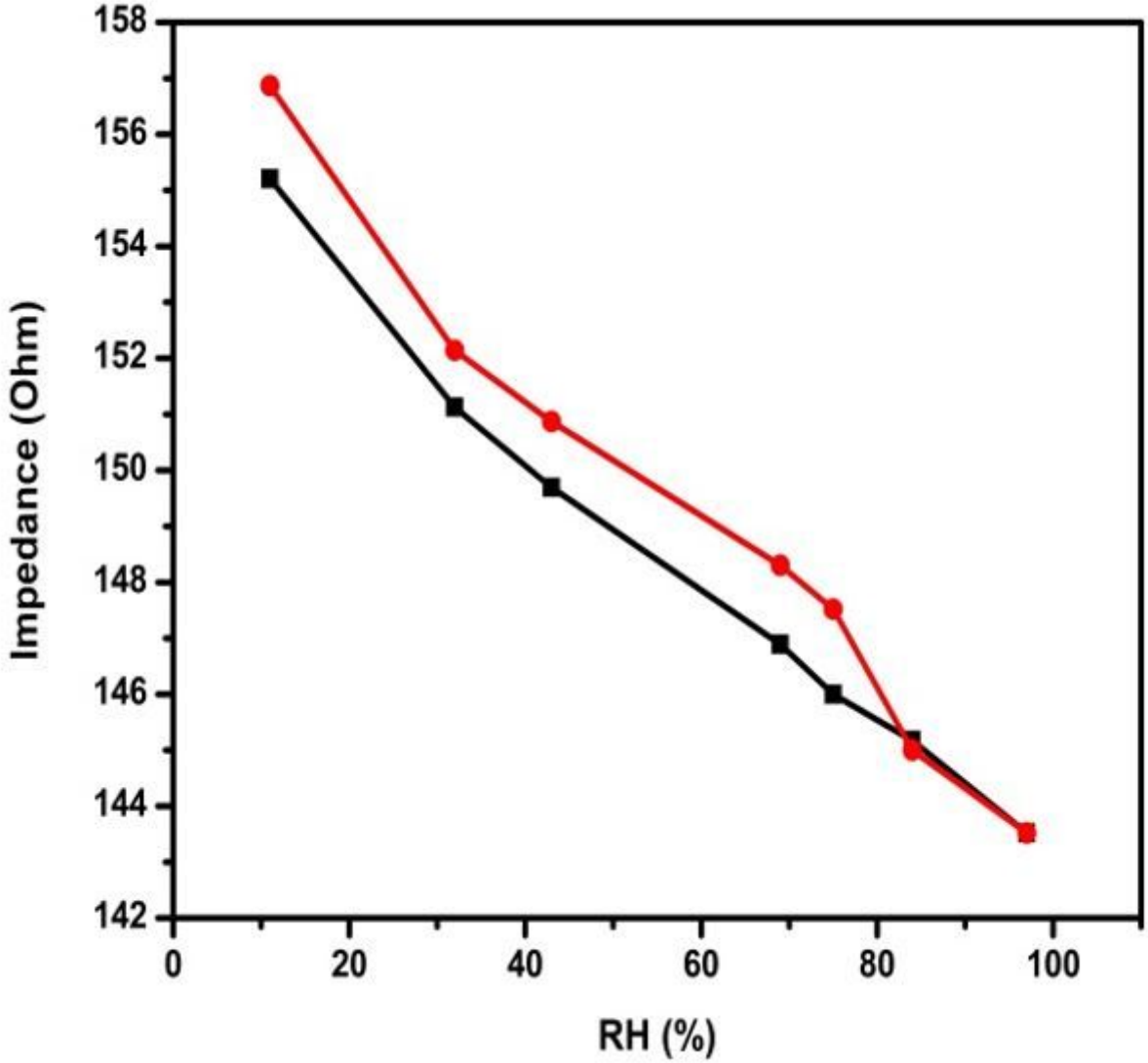

Figure 9

The hysteresis effects due to the adsorption and desorption of water molecule

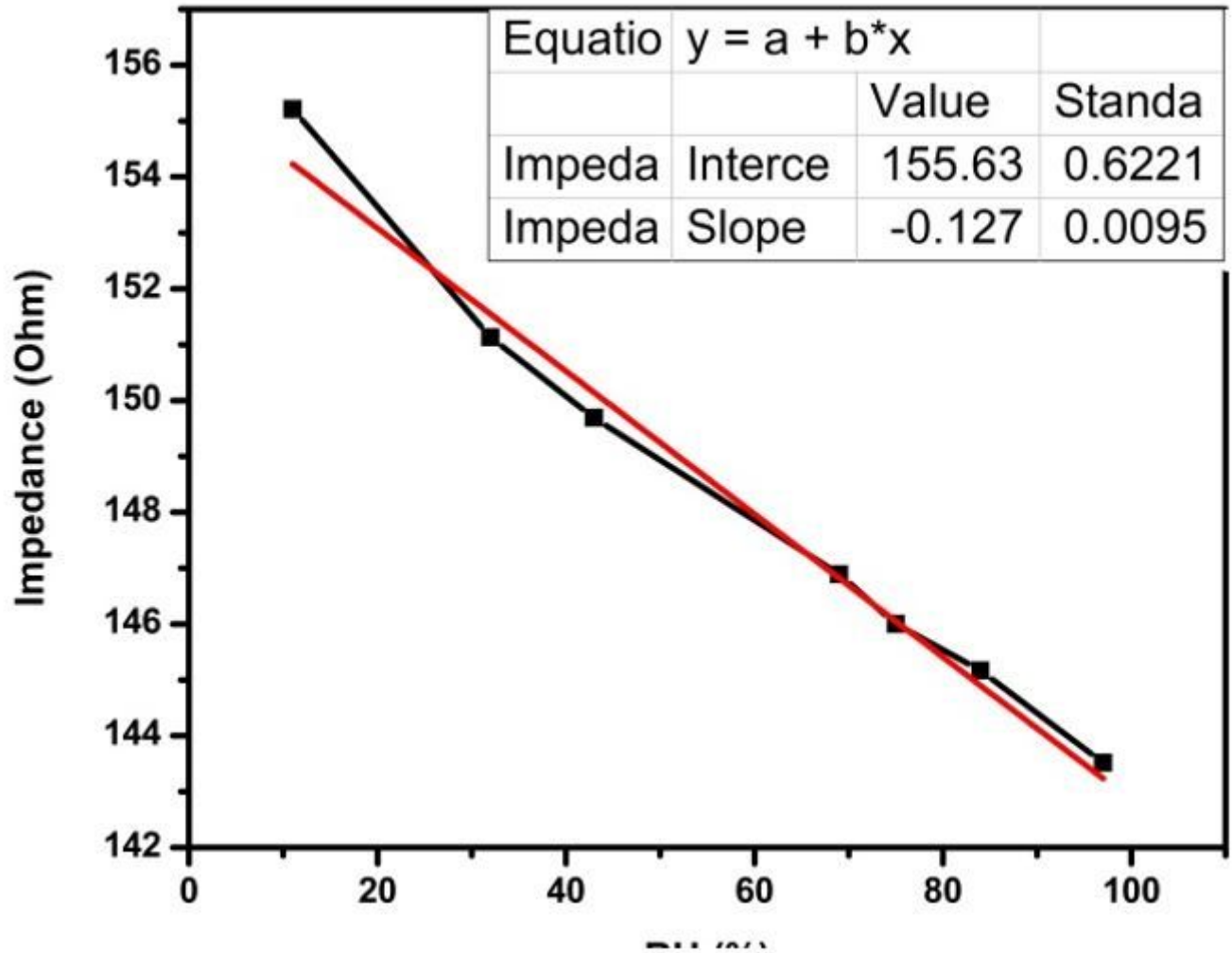

Figure 10

The linear fitting of Co3O4/MWCNTs sensor

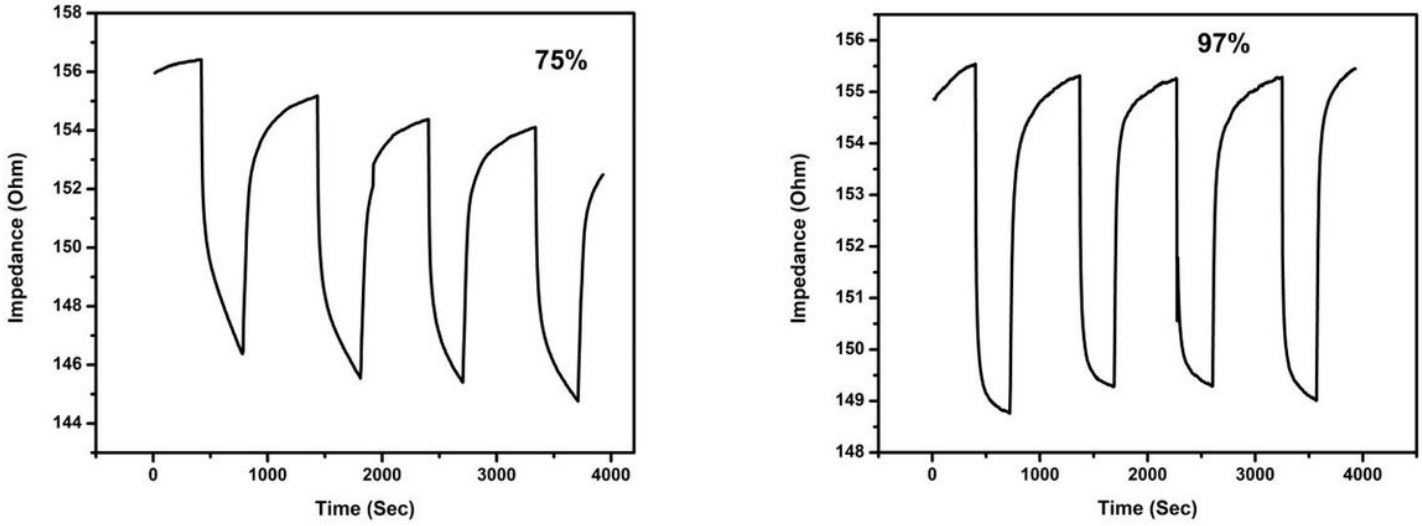

Figure 11

The repeatability of Co3O4/MWCNTs sensor at 75% and 97%

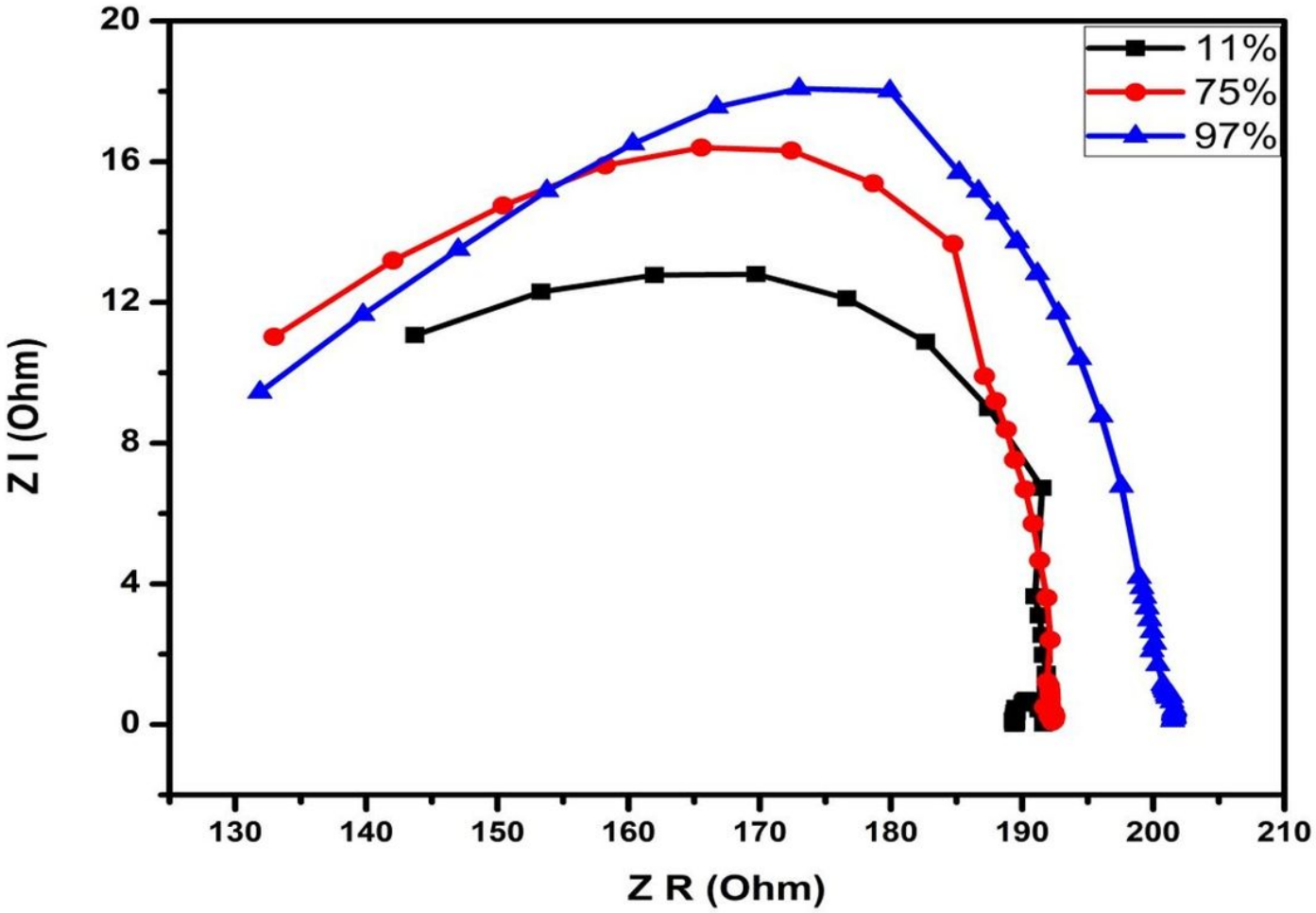

Figure 12

The Cole Cole diagram of humidity sensor at 11%, 75% and 97%